

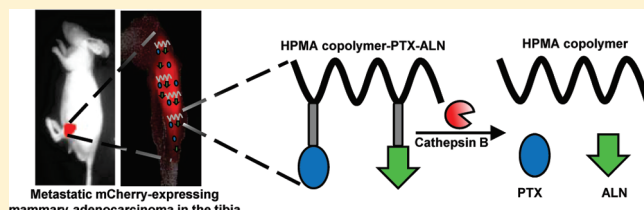
# Antiangiogenic Antitumor Activity of HPMA Copolymer–Paclitaxel–Alendronate Conjugate on Breast Cancer Bone Metastasis Mouse Model

Keren Miller,<sup>†</sup> Anat Eldar-Boock,<sup>†</sup> Dina Polyak,<sup>†</sup> Ehud Segal,<sup>†</sup> Liat Benayoun,<sup>‡</sup> Yuval Shaked,<sup>‡</sup> and Ronit Satchi-Fainaro<sup>\*,†</sup>

<sup>†</sup>Department of Physiology and Pharmacology, Sackler School of Medicine, Room 607, Tel Aviv University, Tel Aviv 69978, Israel

<sup>‡</sup>Department of Molecular Pharmacology, Rappaport Faculty of Medicine, Technion, Israel Institute of Technology, 1 Efron St. Bat Galim, Haifa 31096, Israel

**ABSTRACT:** Polymer therapeutics have shown promise as tumor-targeted drug delivery systems in mice. The multivalency of polymers allows the attachment of different functional agents to a polymeric backbone, including chemotherapeutic and antiangiogenic drugs, as well as targeting moieties, such as the bone-targeting agent alendronate (ALN). We previously reported the conjugation of ALN and the chemotherapeutic drug paclitaxel (PTX) with *N*-(2-hydroxypropyl)methacrylamide (HPMA) copolymer. The *in vitro* physicochemical properties, cancer cytotoxicity and antiangiogenic activity of HPMA copolymer–PTX–ALN conjugate were extensively characterized. The reported results warranted *in vivo* evaluations of the conjugate. In this manuscript, we evaluated the *in vivo* anticancer and antiangiogenic activity of HPMA copolymer–PTX–ALN conjugate. The conjugate exhibited an antiangiogenic effect by decreasing microvessel density (MVD), and inducing apoptotic circulating endothelial cells (CEC) following treatment of the mice. Using intravital imaging system and mCherry-labeled breast cancer cell lines, we were able to monitor noninvasively the progression of orthotopic metastatic tumors injected into the tibia of the mice. HPMA copolymer–PTX–ALN conjugate showed the greatest antitumor efficacy on mCherry-labeled 4T1 mammary adenocarcinoma inoculated into the tibia, as compared with PTX alone or in combination with ALN. Treatment with the bone-targeted polymeric conjugate demonstrated improved efficacy, was better tolerated, and was more easily administered intravenously than the clinically used PTX formulated in Cremophor/ethanol.



**KEYWORDS:** angiogenesis, polymer therapeutics, bone targeting, HPMA copolymer, paclitaxel, alendronate

## ■ INTRODUCTION

Breast cancer almost invariably metastasizes to bones in patients with advanced disease.<sup>1,2</sup> These bone metastases are responsible for much of the disabling morbidity (pain, pathological fractures, hypercalcemia) and mortality.<sup>2</sup> The taxane paclitaxel (PTX), which interferes with microtubule breakdown during cell division, is a known potent cytotoxic agent approved as first line of therapy for metastatic breast cancer.<sup>3–7</sup> Also, it has become evident that ultralow (e.g., picomolar) concentrations of PTX can selectively inhibit endothelial functions relevant to angiogenesis.<sup>8,9</sup> Despite the strong anticancer and antiangiogenic activity, PTX exhibits serious dose-limiting toxicities due to non-specific biodistribution of the drug in both tumors and normal tissues. In addition, PTX is water-insoluble and, therefore, it is formulated in Cremophor EL vehicle, which causes severe allergic, hypersensitivity, and anaphylactic reactions.<sup>10</sup> Progression to a PTX-resistant phenotype is also seen in the majority of patients following initial response to treatment.<sup>4,7,11,12</sup> To address these problems, a variety of formulations and delivery systems are being investigated to increase the availability at the tumor site and maximize the therapeutic efficacy while minimizing the side effects of PTX.<sup>13–15</sup> During the past decade, tremendous efforts

have been invested in drug targeting using various delivery systems. These nanoscaled delivery systems include polymers, micelles, dendrimers and liposomes. Drug conjugation with polymers is one of the most promising and investigated approaches for cancer therapy.<sup>16–21</sup> Drug conjugation with water-soluble polymers restricts their passage through the blood brain barrier, protects the drugs from degradation and inactivation, increases their accumulation at the tumor site, and thus decreases side effects. Polymer–drug conjugates injected systemically accumulate in tumor tissues by escaping through the abnormally leaky tumor blood vessels, a phenomenon known as the enhanced permeability and retention (EPR) effect.<sup>22</sup> In addition to such passive targeting of polymer–drug conjugates, active targeting can be combined by introducing a recognition specific moiety.

**Special Issue:** Molecular Pharmaceutical Strategies for Improved Treatment of Musculoskeletal Diseases

**Received:** February 22, 2011

**Accepted:** May 5, 2011

**Revised:** April 26, 2011

**Published:** May 05, 2011

This dual targeting should provide better and more efficient tissue specific accumulation of the drug. Alendronate (ALN), an aminobisphosphonate, is commonly used for prevention and treatment of osteoporosis, bone metastases and myelomatous bone disease. ALN possesses high binding affinity to the bone mineral hydroxyapatite (HA), and therefore it can be used also as a bone-targeting moiety.<sup>23–25</sup>

We previously reported the synthesis of a polymer conjugate composed of PTX and ALN.<sup>26</sup> Both drugs were conjugated with *N*-(2-hydroxypropyl)methacrylamide (HPMA) copolymer. ALN facilitates the delivery of PTX to the bones, and the conjugation with a polymer provides targeting to tumor tissue within the bones. PTX and ALN were both conjugated with HPMA copolymer through the tetrapeptide Gly-Phe-Leu-Gly (GFLG)-ONp. In addition, PTX was conjugated through a consecutive linker, Phe-Lys-*p*-aminobenzyl carbonate (FK-PABC). This dipeptide-PABC linker provides a stable conjugation chemistry of PTX with HPMA copolymer by the carbonate linkage. Both GFLG and FK linkers are cleaved by the lysosomal enzyme cathepsin B, an overexpressed and secreted enzyme in tumor endothelial and epithelial cells.<sup>27–30</sup> The resulting conjugate is water-soluble and, therefore, can be administered in aqueous solution as opposed to free PTX. This advantage abrogates the need for the solubilizing toxic agent Cremophor EL. The physicochemical properties of HPMA copolymer-PTX-ALN conjugate were previously characterized extensively *in vitro*.<sup>26</sup> The hydrodynamic diameter of the nanoscaled HPMA copolymer-PTX-ALN conjugate was ~100 nm. HPMA copolymer-PTX-ALN conjugate was efficiently cleaved by cathepsin B and released free PTX. Our nanoscaled conjugate was shown to bind to HA, a model mineral mimicking bone tissue. The conjugate inhibited the proliferation of PC3 human prostate adenocarcinoma cell line, demonstrating that the conjugation with HPMA copolymer did not impair the cytotoxicity of PTX. Furthermore, HPMA copolymer-PTX-ALN conjugate demonstrated antiangiogenic activity by inhibiting the capillary-like tube formation, migration and proliferation of endothelial cells.

In this current study, we evaluated the antiangiogenic, anticancer and safety profiles of HPMA copolymer-PTX-ALN conjugate *in vitro* and *in vivo* on a murine syngeneic model of mammary adenocarcinoma.

## ■ EXPERIMENTAL SECTION

**Materials.** HPMA copolymer-Gly-Phe-Leu-Gly-ONp incorporating 10 mol % of the methacryloyl-Gly-Phe-Leu-Gly-*p*-nitrophenol ester monomer units was obtained from Polymer Laboratories (Church Stretton, U.K.). The HPMA copolymer-GFLG-ONp has a molecular weight of 31,600 Da and a polydispersity of 1.66. PTX and ALN were purchased from Alcon Biosciences Ltd. (Mumbai, India; Petrus Chemicals and Materials Ltd., Herzliya, Israel). Dulbecco's modified Eagle's medium (DMEM), RPMI 1640, fetal bovine serum (FBS), penicillin, streptomycin, nystatin, L-glutamine, Hepes buffer, sodium pyruvate, and fibronectin were from Biological Industries Ltd. (Kibbutz Beit Haemek, Israel). EGM-2 medium was from Cambrex (Walkersville, MD, USA). Matrigel matrix was from BD Biosciences, U.S.A. Antifade mounting medium was from Biomedica Corp. (Foster City, CA, USA). Peroxidase block was purchased from Merck, Germany. Primary rat anti-murine CD34 antibody (MEC 14.7) was from Abcam, (Cambridge, MA, USA). Rabbit anti-rat antibody, anti-rabbit horseradish

peroxidase-conjugated antibody (ABC detection kit) and ImmPACT DAB diluent kit were from Vector Laboratories (Burlingame, CA, USA). pEGFPLuc plasmid was from Clontech (Mountain View, CA, USA). Nuclear staining was from Procount, BD Pharmingen (San Jose, CA, USA). 7-Aminoactinomycin D (7AAD) was from Chemicon (Billerica, MA, USA). Dextran (MW ~70000) and all other chemical reagents, including salts and solvents, were purchased from Sigma-Aldrich (Rehovot, Israel). All reactions requiring anhydrous conditions were performed under an Ar or N<sub>2</sub> atmosphere. Chemicals and solvents were either AR grade or purified by standard techniques.

### Synthesis of HPMA Copolymer-PTX-ALN Conjugates.

The conjugation of PTX with HPMA copolymer was performed as previously described.<sup>26</sup> Briefly, PTX was first attached with the FK-PABC linker and then was conjugated to HPMA copolymer-GFLG-ONp. L-Boc-Phe-ONp was conjugated to L-Lys(aloc)-OH. Amidation with 4-aminobenzyl alcohol (PABA) was then followed with activation with *p*-nitrophenol, which was then reacted with PTX. Deprotection of the Boc group afforded the free amine, which was then conjugated with HPMA copolymer-GFLG-ONp. Then amidation of HPMA copolymer-GFLG-PTX-FK was performed with an excess of ALN. Finally, deprotection of the aloc group of the amine residue of Lys affords the desired HPMA copolymer-PTX-ALN. Drug loading and hydrodynamic diameter were determined as previously described.<sup>26</sup>

**Red Blood Cells Lysis Assay.** Red blood cell (RBC) lysis was performed as previously described.<sup>31</sup> Briefly, 2% w/w rat RBC solution was incubated with serial dilutions of HPMA copolymer-PTX-ALN conjugate, combination of free PTX plus ALN at equivalent concentrations, HPMA copolymer and PTX-vehicle (1:1:8 ethanol:Cremophor EL:saline) for 1 h at 37 °C. Negative controls were PBS and dextran (MW ~70000), while positive controls were 1% w/v solution of Triton X-100 (100% lysis) and polyethyleneimine (PEI). Following centrifugation, the supernatant was drawn off and its absorbance measured at 550 nm using a microplate reader (Genios, TECAN). The results were expressed as percentage of hemoglobin released relative to the positive control (Triton X-100).

**Cell Culture.** MDA-MB-231 human mammary adenocarcinoma cell line and 4T1 murine mammary adenocarcinoma cell line were purchased from the American Type Culture Collection (ATCC). MDA-MB-231 cells were cultured in DMEM supplemented with 10% FBS, 100 µg/mL penicillin, 100 U/mL streptomycin, 12.5 U/mL nystatin and 2 mM L-glutamine. 4T1 cells were cultured in RPMI 1640 supplemented with 10% FBS, 100 µg/mL penicillin, 100 U/mL streptomycin, 12.5 U/mL nystatin and 2 mM L-glutamine, 10 mM Hepes buffer, and 1 mM sodium pyruvate. Cells were grown at 37 °C; 5% CO<sub>2</sub>.

**Generation of mCherry-Infected 4T1 Murine Mammary Adenocarcinoma Cell Line.** mCherry was subcloned from pART7-mCherry (kindly provided by A. Avni from Tel Aviv University), into pQCXIP (Clontech). Human embryonic kidney 293T (HEK 293T) cells were cotransfected with pQC-mCherry and the compatible packaging plasmids (pMD.G. VSVG and pGag-pol.gpt). Forty-eight hours following transfection, the pQC-mCherry retroviral particles containing supernatant were collected. 4T1 murine mammary adenocarcinoma cells were infected with the retroviral particle media, and 48 h following the infection, mCherry positive cells were selected by puromycin resistance.

**Cell Viability Assay.** 4T1 and MDA-MB-231 cells were plated onto a 96 well plate (5 × 10<sup>3</sup> cells/well) in RPMI 1640, or

DMEM supplemented with 5% FBS and incubated for 24 h (37 °C; 5% CO<sub>2</sub>). Following 24 h of incubation, medium was replaced with RPMI 1640 or DMEM containing 10% FBS. Cells were challenged with the combination of free PTX plus ALN, each drug alone, and HPMA copolymer–PTX–ALN conjugate at serial concentrations for 72 h. Cell viability was measured by Thiazolyl Blue Tetrazolium Blue (MTT) (Sigma-Aldrich, Israel). A 30  $\mu$ L solution of 2 mg/mL MTT was added to wells containing cells that were grown at 100  $\mu$ L of medium for 5 h incubation at 37 °C; 5% CO<sub>2</sub>. Following incubation, medium was replaced with dimethyl sulfoxide (DMSO) until blue color was developed. Viability was measured spectrophotometrically at 560 nm.

**Ethics Statement.** All animal procedures were performed in compliance with Tel Aviv University, Sackler School of Medicine guidelines and protocols approved by the Institutional Animal Care and Use Committee.

**In Vivo Safety Profile.** The safety profile of HPMA copolymer–PTX–ALN conjugate was carried out *in vivo* on female Balb/c mice with a low metronomic (antiangiogenic) dosing schedule. Balb/c mice were injected ip every day for up to 10 days, with the combination of free PTX (4 mg/kg) plus ALN (2.5 mg/kg), each drug alone, HPMA copolymer–PTX–ALN conjugate at equivalent PTX and ALN concentrations and saline and PTX–vehicle, that were used as controls. Following 10 days of treatment, the dosing schedule was increased to 8 mg/kg PTX and 5 mg/kg ALN. On day 17, blood samples were collected and WBC were counted. For the maximum tolerated dose (MTD), severe combined immunodeficiency (SCID) mice were injected 5 times every other day iv with the combination of free PTX (15 mg/kg) plus ALN (9.5 mg/kg), free PTX, HPMA copolymer–PTX–ALN conjugate at equivalent PTX and ALN concentrations and saline, and PTX–vehicle. On day 13, blood samples were collected and WBC were counted.

**White Blood Cell (WBC) Counts.** Blood was obtained from anesthetized mice by retro-orbital sinus bleeding. Twenty four hours after treatment, blood was collected in tubes containing 0.1 M EDTA to avoid clotting. Samples were counted no longer than five minutes after blood was drawn from mice. Ten microliters of blood samples was mixed with 90  $\mu$ L of track solution (1% acetic acid in DDW), and cells were counted by a Z1 Coulter particle counter (Beckman Coulter). Data is expressed as mean  $\pm$  SEM.

**Evaluation of Antitumor Activity of HPMA Copolymer–PTX–ALN Conjugate.** Balb/c female mice were injected intratibia with  $4 \times 10^5$  mCherry-labeled 4T1 cells. Therapy was initiated one day after tumor cell inoculation. For the treatments, 100  $\mu$ L of free PTX (15 mg/kg), free ALN (9.5 mg/kg), combination of free PTX plus ALN, PTX–vehicle, saline, or HPMA copolymer–PTX–ALN conjugate was injected intravenously (iv) via the tail vein, every other day ( $n = 6$  mice/group). Tumor progression was monitored noninvasively by a CRI Maestro intravital imaging system. At termination, tibias were removed and analyzed. Data is expressed as mean  $\pm$  SEM.

**Immunohistochemistry.** Tumor samples were fixed with 4% paraformaldehyde, following decalcification in EDTA and paraffin embedding by the standard procedure. Immunohistochemistry of tumor in the tibia was performed using 4  $\mu$ m thick formalin-fixed, paraffin-embedded tissue sections. Paraffin sections were deparaffinized, rehydrated, and stained by hematoxylin and eosin (H&E). For Caspase 3, PCNA, and CD34 staining, slides were deparaffinized and pretreated with 10 mM citrate, pH 6.0 for 20

min in a steam pressure cooker (Decloaking Chamber, BioCare Medical, Walnut Creek, CA, USA). All further steps were performed at RT in a hydrated chamber. Slides were covered with peroxidase block (Merck, Germany) for 10 min to quench endogenous peroxidase activity, followed by incubation with 2% of horse serum in 50 mM Tris-HCl, pH 7.4, for 30 min to block nonspecific binding sites. Primary rat anti-murine CD34 antibody (MEC 14.7 1:50 dilution; Abcam, Cambridge, MA, USA), rabbit anti-murine caspase 3 antibody (C-9661S 1:200 dilution; Cell Signaling), and biotin anti-murine PCNA (PC-10 1:1000 dilution, Biolegend) were applied in 1% rabbit serum albumin in Tris-HCl, pH 7.4 at 4 °C overnight. Slides were washed in 50 mM Tris-HCl, pH 7.4, and rabbit anti-rat antibody (1:750 dilution; Vector Laboratories, CA, USA) was applied for 30 min. Following further washing, immunoperoxidase staining was developed using HistoMark TrueBlue peroxidase system (KPL, USA) per the manufacturer's instructions and counterstained with safranin. For biotinylated PCNA antibody, color development was done using Vectastain Elite ABC Kit (Vector Laboratories) and Sigma Fast Kit (Sigma-Aldrich) with counterstaining by Mayer hematoxylin. Microvessel density (MVD) was calculated as previously described.<sup>32</sup>

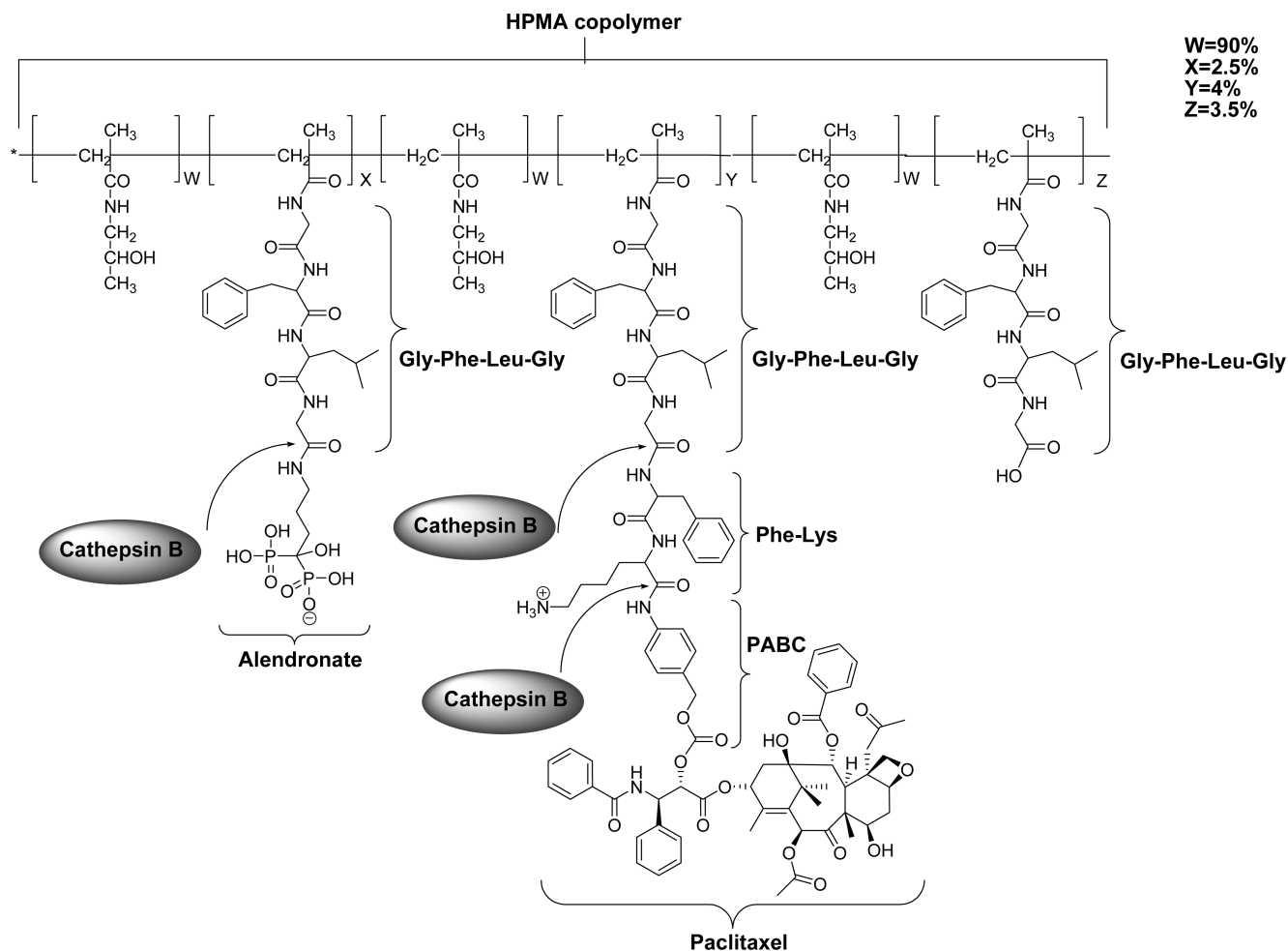
**Measurement of Circulating Endothelial Cells (CEC) by Flow Cytometry.** Blood was obtained from anesthetized mice by retro-orbital sinus bleeding. CEC were quantitated using flow cytometry, as described previously.<sup>33</sup> Briefly, 24 h after treatment, blood was collected in tubes containing EDTA to avoid clotting. Monoclonal antibodies were used to detect CEC population with the following antigenic phenotypes: CD13+/VEGFR2+/CD45–/dim. Nuclear staining was used in some experiments to exclude platelets or cellular debris. 7-Amino-actinomycin D (7AAD) was used to distinguish apoptotic and dead cells from viable cells. After red cell lysis, cell suspensions were analyzed and at least 200,000 cells per sample were acquired. Analyses were considered informative when an adequate number of events (i.e., >50, typically 50–150) was collected in the CEC enumeration gate in untreated control animals. Percentages of stained cells were determined and compared with appropriate negative controls. Positive staining was defined as being greater than nonspecific background staining. Flow cytometry studies were performed on a Cyan ADP flow cytometer (Beckman Coulter) and analyzed with Summit (Beckman Coulter) software. All monoclonal antibodies were purchased from BD Biosciences and used for flow cytometry analysis in accordance with the manufacturer's protocols. Data is expressed as mean  $\pm$  SEM.

**Statistical Methods.** *In vitro* data from proliferation assays on 4T1 and MDA-MB-231 cells is expressed as mean  $\pm$  standard deviation (SD). *In vivo* data of antitumor activity is expressed as mean  $\pm$  SEM. Statistical significance was determined using an unpaired *t*-test.  $P < 0.05$  was considered statistically significant. All statistical tests were two-sided.

## ■ RESULTS

**Synthesis and Characterization of HPMA Copolymer–PTX–ALN Conjugate.** The chemical structure of HPMA copolymer–PTX–ALN conjugate is presented in Scheme 1. Batches of conjugate synthesized for this study revealed similar physicochemical properties as reported for previous batches.<sup>26</sup> The resulting conjugate was water-soluble, its hydrodynamic

**Scheme 1. Chemical Structure of HPMA Copolymer–PTX–ALN Conjugate and Cleavage Mechanism of PTX and ALN by Cathepsin B**



diameter in aqueous solution was  $\sim 100$  nm, and PTX and ALN loading were 4 and 2.5 mol %, respectively.

**HPMA Copolymer–PTX–ALN Conjugate Inhibits the Proliferation of the Human MDA-MB-231 and Murine 4T1 Mammary Adenocarcinoma Cancer Cell Lines.** HPMA copolymer–PTX–ALN conjugate cytotoxicity was demonstrated previously on the human PC3 prostate adenocarcinoma cell line.<sup>26</sup> Aiming to be used as breast cancer bone metastasis inhibitor, the effect of HPMA copolymer–PTX–ALN conjugate on breast cancer cell lines was evaluated. HPMA copolymer–PTX–ALN conjugate exhibited cytotoxic effects on both 4T1 (Figure 1A) and MDA-MB-231 (Figure 1B) cell lines with an  $IC_{50}$  of  $\sim 200$  nM. HPMA copolymer served as control and was nontoxic at all the concentrations tested. ALN alone was nontoxic at all concentrations tested.  $IC_{50}$  for free PTX and combination of free PTX plus ALN was  $\sim 10$  nM for both 4T1 and MDA-MB-231 cell lines. It should be noted that the addition of equivalent concentrations of ALN in combination with PTX had no benefit over PTX alone in inhibiting 4T1 and MDA-MB-231 cell growth.

**HPMA Copolymer–PTX–ALN Conjugate Is Hemocompatible.** The hemocompatibility of HPMA copolymer–PTX–ALN conjugate was evaluated *ex vivo*. Rat RBC were incubated with the

different compounds, and the lysis assay was performed. The results clearly show that HPMA copolymer–PTX–ALN conjugate is not hemolytic *ex vivo* at concentrations up to 5 mg/mL (the estimated blood concentration following *in vivo* administrations is about 0.5 mg/mL). PEI, which served as control, caused 80% hemolysis. The cytotoxicity of PTX–vehicle that contains Cremophor EL (1:1:8 ethanol:Cremophor EL:saline) is known on normal nonproliferating cells,<sup>34</sup> and indeed, a slight RBC hemolysis of  $\sim 8\%$  was observed in RBC incubated with PTX–vehicle. A slight hemolysis was also observed in RBC incubated with the combination of free PTX plus ALN at the highest concentration of 5 mg/mL (Figure 2).

**In vivo Safety Profile.** The safety profile of HPMA copolymer–PTX–ALN conjugate was carried out *in vivo* on female Balb/c and SCID mice with low metronomic (antiangiogenic) dosing or at MTD schedules, respectively. Low metronomic, antiangiogenic dosing schedule can indicate the long-term effect of the conjugate and the free drugs *in vivo*. Balb/c mice were injected every day for up to 10 days, with the different compounds. As expected, no significant body weight loss occurred during that period. Following 10 days of treatment, the dosing schedule was doubled. Body weight gradually started to decrease in mice treated with PTX in combination with ALN and reached

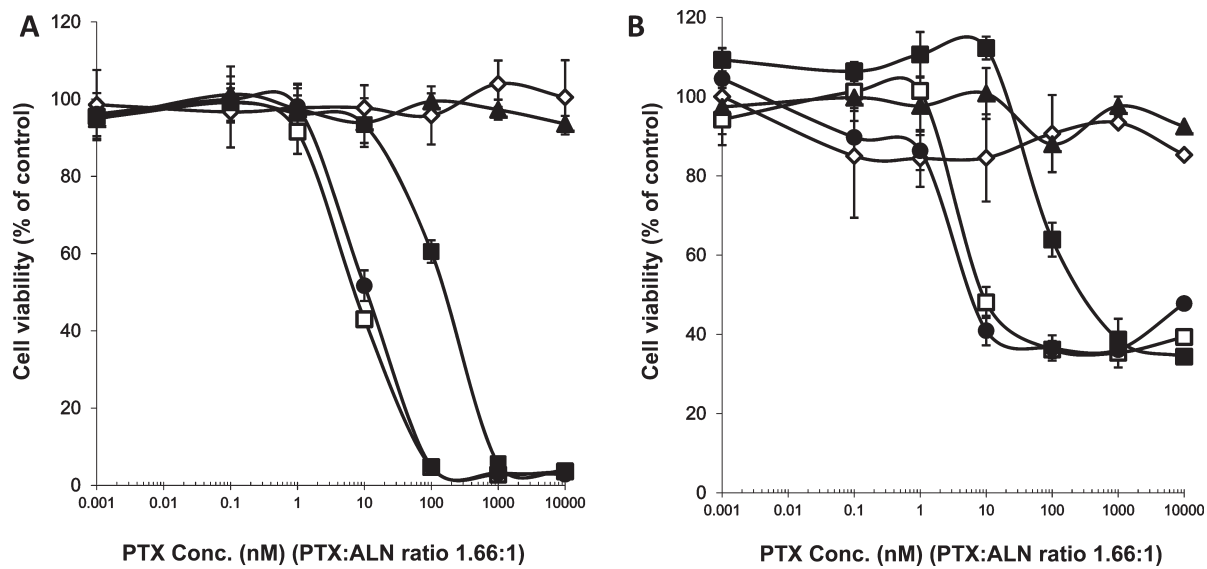


**Figure 1.** HPMA copolymer-PTX-ALN conjugate inhibits the proliferation of murine 4T1 and human MDA-MB-231 mammary adenocarcinoma cancer cell lines. 4T1 (A) and MDA-MB-231 (B) cells were incubated with the combination of free PTX plus ALN (open squares), free PTX (closed circles), free ALN (closed triangles), HPMA copolymer-PTX-ALN conjugate (closed squares), and with HPMA copolymer (open diamonds) for 72 h. Data represents mean  $\pm$  SD. The X-axis is presented at a logarithmic scale.

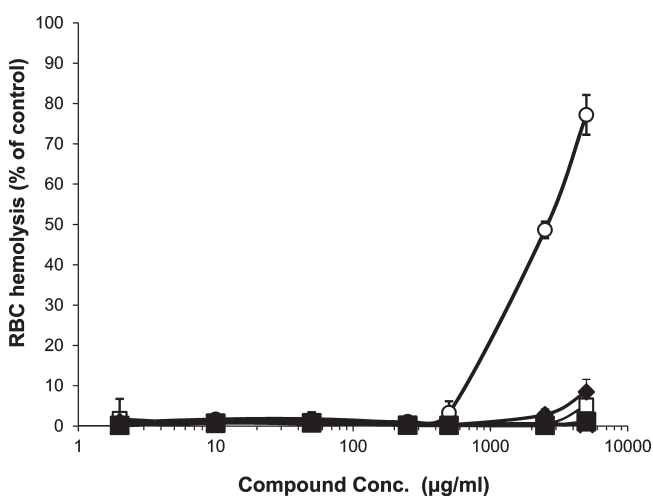


**Figure 2.** HPMA copolymer-PTX-ALN conjugate is hemocompatible. Rat RBC were incubated for 1 h with HPMA copolymer-PTX-ALN conjugate (closed squares), the combination of free PTX plus ALN at equivalent concentrations (open squares), PEI (open circles), PTX-vehicle (closed diamonds), and HPMA copolymer (open diamonds). Results are presented as % of hemoglobin released produced by the different compounds relative to positive control (Triton X-100). Data represents mean  $\pm$  SD. Due to similar values, some symbols overlap.

~5% loss. Treatment with HPMA copolymer-PTX-ALN conjugate did not cause body weight loss (Figure 3A). On day 17, blood samples were collected and WBC were counted. Mice treated with HPMA copolymer-PTX-ALN conjugate had normal levels of WBC, whereas mice treated with PTX alone, PTX in combination with ALN, and PTX-vehicle (1:1:8 ethanol:Cremophor EL:saline) exhibited a significant decrease in WBC counts (Figure 3B). Furthermore, motor coordination and balance performance were not affected in mice treated with the conjugate, indicating that the conjugate is not neurotoxic

(data not shown). For the MTD schedule, SCID mice were injected with the different compounds. On day 12, a significant body weight loss was recorded in mice treated with free PTX plus ALN, reaching 17% decrease. Body weight was recovered quickly after treatment withdrawal. Mice treated with equivalent concentrations of HPMA copolymer-PTX-ALN conjugate did not lose weight (Figure 3C). Blood samples collected on day 13 were evaluated for WBC counts and were at normal range in mice treated with HPMA copolymer-PTX-ALN conjugate. Mice treated with PTX alone had a significant decrease in WBC counts (Figure 3D).

**Evaluation of Antitumor Efficacy and Toxicity Profile of HPMA Copolymer-PTX-ALN Conjugate in Mice Bearing 4T1-mCherry Murine Mammary Adenocarcinoma in the Tibia.** We previously showed improved antitumor effect of HPMA copolymer-PTX-ALN conjugate administered at low metronomic (antiangiogenic) dosing schedule on the PTX-resistant DA3 murine mammary adenocarcinoma in bones.<sup>35</sup> We next evaluated its effect at the MTD schedule of PTX. Using mCherry-labeled 4T1 murine mammary adenocarcinomas and intravital fluorescence imaging system we could monitor non-invasively tumor growth in tibias. Balb/c female mice were treated iv with the different compounds at MTD schedule. Although tumor progression was not halted, it was significantly inhibited in mice treated with free PTX, the combination of free PTX plus ALN, and with HPMA copolymer-PTX-ALN conjugate, as compared to control-treated mice. The superiority of our HPMA copolymer-PTX-ALN conjugate over the combination of free PTX plus ALN became evident when injected *in vivo*. On day 15, when mice were euthanized, HPMA copolymer-PTX-ALN conjugate inhibited tumor growth by 60% (compared with mice treated with saline), whereas combination of free ALN plus PTX resulted in tumor growth inhibition of 37% (compared with mice treated with PTX-vehicle) (Figures 4A and 4B).

Toxicities were assessed by analyzing effects on animal behavior, body weight change, and WBC counts. In all these parameters

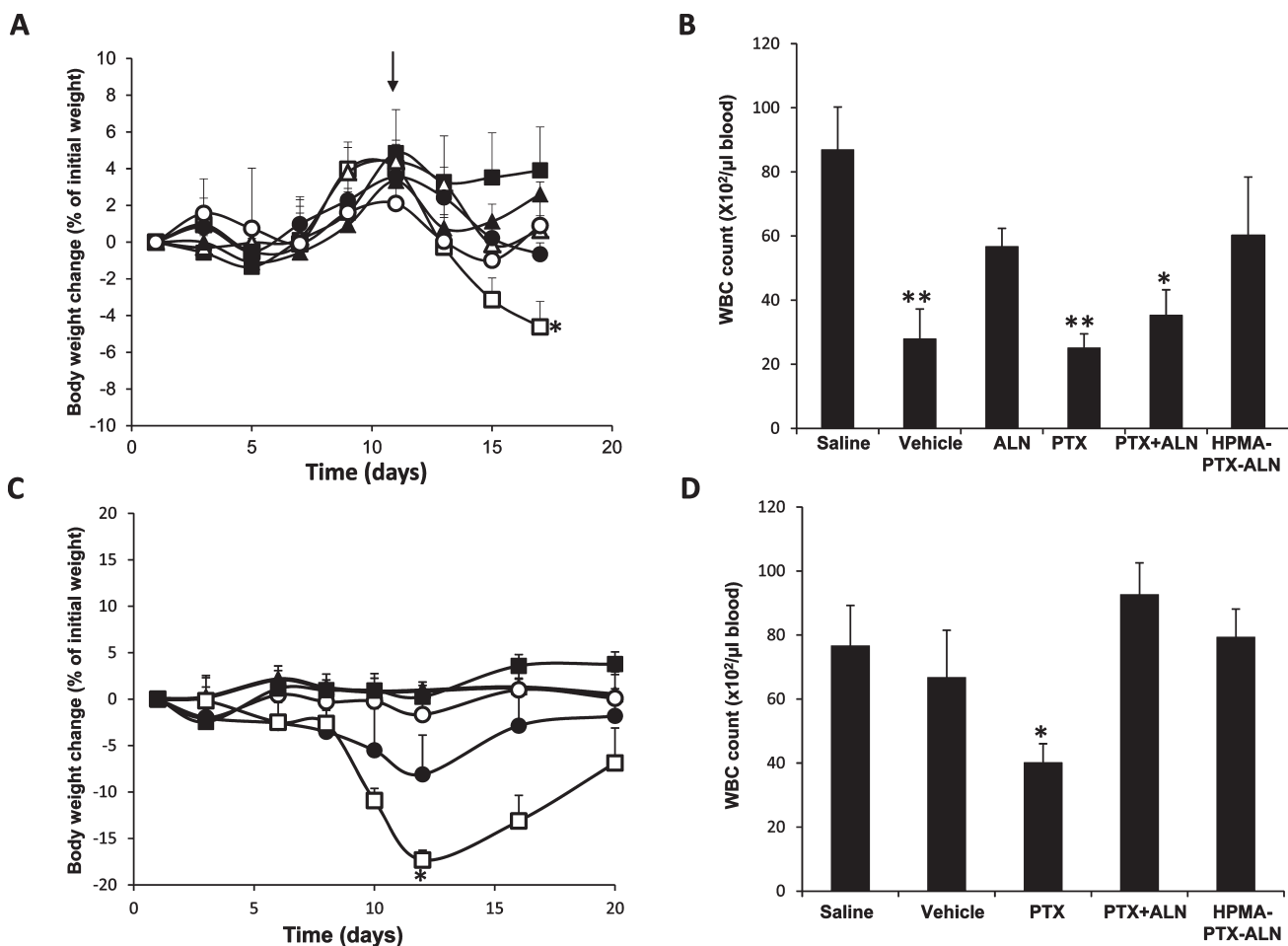


**Figure 3.** HPMA copolymer-PTX-ALN conjugate is nontoxic at low metronomic (antiangiogenic) dosing or MTD schedules. (A) Balb/c mice were administered ip, every day, for 10 days with low metronomic dosing schedule of 4 mg/kg PTX (closed circles), 2.5 mg/kg ALN (open triangles), combination of free ALN plus PTX (open squares), HPMA copolymer-PTX-ALN conjugate at equivalent concentrations (closed squares), and saline (closed triangles) or PTX-vehicle (open circles) that were used as controls. Following 10 days of treatment (arrow), the dosing schedule was increased to 8 mg/kg PTX and 5 mg/kg ALN. Mice were monitored every other day for body weight change (presented as % change from initial weight). (B) WBC counts of blood samples collected on day 17 from Balb/c mice injected with low metronomic dosing schedule. (C) SCID mice were administered iv, every other day (5 injections), with MTD schedule of 15 mg/kg PTX (closed circles), combination of free ALN plus PTX (open squares), HPMA copolymer-PTX-ALN conjugate at equivalent concentrations (closed squares), and saline (closed triangles) or PTX-vehicle (open circles) that were used as controls. Mice were monitored every other day for body weight change (presented as % change from initial weight). (D) WBC counts of blood samples collected on day 13 from SCID mice injected with MTD schedule. Data represent mean  $\pm$  SEM of five mice per group. \* $P$  < 0.05, \*\* $P$  < 0.01.  $P$  value of mice treated with HPMA copolymer-PTX-ALN conjugate was analyzed against saline control mice.  $P$  value of free PTX or combination of free PTX plus ALN was analyzed against control mice treated with PTX-vehicle.

there was no significant toxicity observed in mice treated with the conjugate (Figures 4C and 4D). WBC counts in mice treated with HPMA copolymer-PTX-ALN conjugate, the combination of free PTX plus ALN, or PTX-vehicle were at the normal range and similar to those of control mice injected with saline. Only mice treated with PTX exhibited significant reduction in WBC counts (Figure 4D).

Representative histologic sections of H&E staining through the proximal tibial metaphysis demonstrate that, in control and in mice treated with free PTX or ALN, tumor filled the bone marrow space and destroyed both trabecular and cortical bone. In contrast, most of the HPMA copolymer-PTX-ALN treated mice had intact cortical and trabecular bone (Figure 5A).

On immunohistochemical analysis of paraffin-embedded sections, no change in stained proliferating cell nuclear antigen (PCNA) was recorded in all treatments (Figure 5B). The degree

of apoptosis, assessed by staining of cleaved caspase-3, was increased by  $\sim$ 3- and  $\sim$ 3.5-fold in mice treated with HPMA copolymer-PTX-ALN conjugate and the combination of free PTX plus ALN, respectively (Figure 5C). CD34 Staining showed  $\sim$ 50% reduction in MVD in tumors of mice treated with HPMA copolymer-PTX-ALN conjugate, the combination of free PTX plus ALN, and each free drug, as compared with control mice (Figure 5D).

**HPMA Copolymer-PTX-ALN Conjugate Increases Apoptotic CEC Levels.** Following the *in vivo* Miles vascular permeability assay and our previous *in vitro* results demonstrating the antiangiogenic activity of HPMA copolymer-PTX-ALN conjugate, we performed a CEC count analysis on the 4T1-mCherry murine mammary adenocarcinoma in the tibia mouse model. Circulating endothelial cells (CEC), usually apoptotic in healthy subjects and more viable in cancer patients, are likely to represent

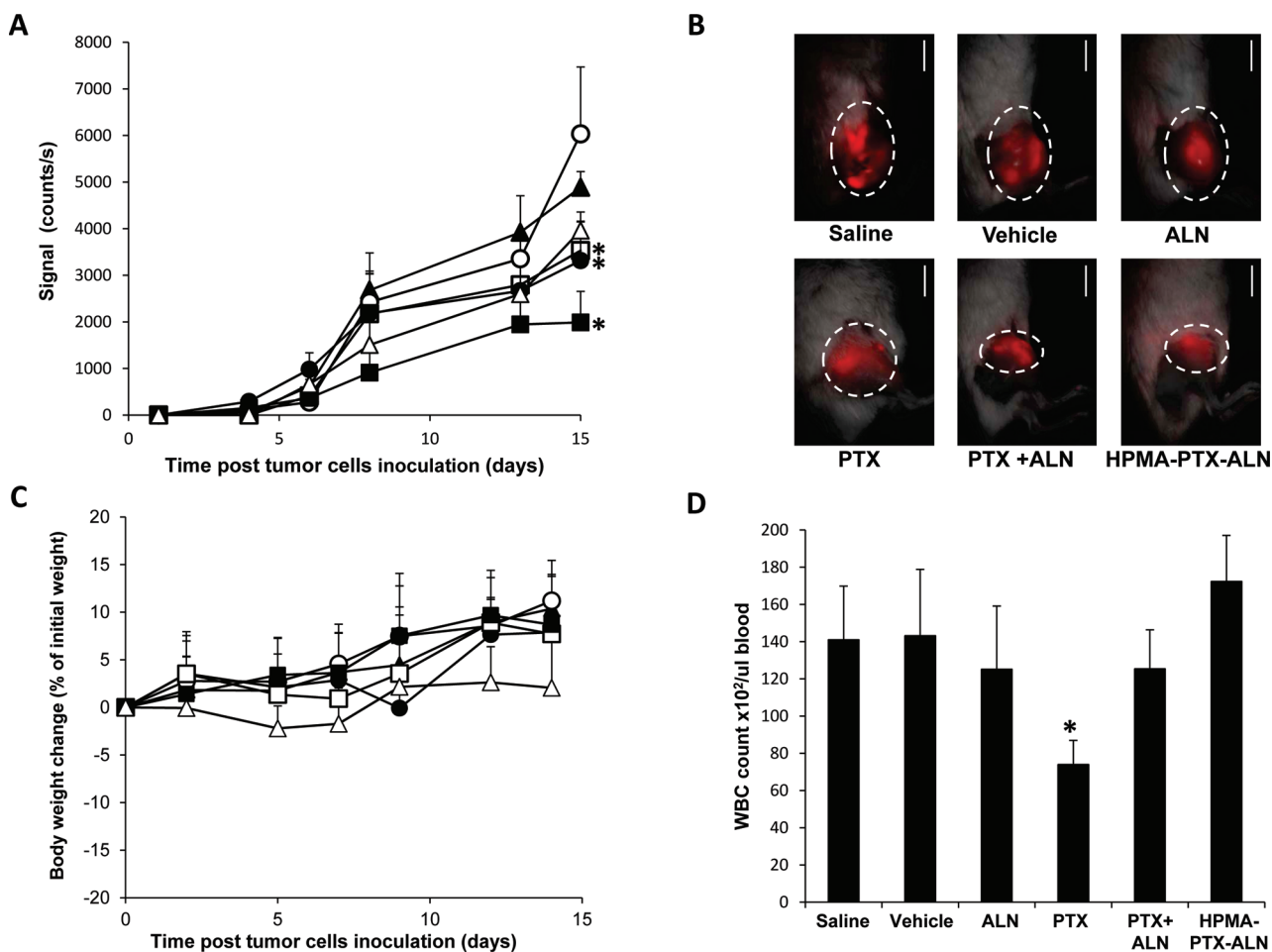


**Figure 4.** HPMA copolymer–PTX–ALN conjugate inhibits 4T1-mCherry mammary adenocarcinoma in the tibia. Mice bearing 4T1-mCherry mammary adenocarcinoma inoculated in the tibia were administered iv, every other day with 15 mg/kg PTX (closed circles), 9.5 mg/kg ALN (open triangles), combination of free ALN plus PTX (open squares), HPMA copolymer–PTX–ALN conjugate at equivalent concentrations (closed squares), and saline (closed triangles) or PTX–vehicle (open circles) that were used as controls. (A) Antitumor efficacy measured by intravital noninvasive fluorescence imaging of 4T1-mCherry adenocarcinomas in the tibia. (B) Fluorescence images of 4T1-mCherry adenocarcinomas in the tibia. Scale bar represents 15 mm. (C) Body weight change (presented as % change from initial weight). (D) WBC counts from blood samples collected on day 11. Data represent mean  $\pm$  SEM of six mice per group. \* $P < 0.05$  value of mice treated with HPMA copolymer–PTX–ALN conjugate was analyzed against saline control mice. \* $P < 0.05$  value of free PTX or combination of free PTX plus ALN was analyzed against control mice treated with PTX–vehicle.

an indirect marker of vessel damage and/or turnover and remodeling.<sup>36–38</sup> Using multiparametric flow cytometry, we analyzed the apoptotic and total number of endothelial cells circulating in the blood. Following all treatments, except the conjugate, there was no significant difference in apoptotic CEC counts in the blood. However, in mice treated with HPMA copolymer–PTX–ALN conjugate there was a significant increase in apoptotic CEC counts in the blood (Figure 6).

## ■ DISCUSSION

Polymer therapeutics is one of the promising approaches to treat cancer. Not only that conjugation of drugs with polymers increases water-solubility, a renowned limitation associated with many chemotherapeutic drugs such as PTX, it can also prolong the circulation time, achieve controlled and sustained drug release and improve tumor accumulation, thereby maximizing the therapeutic index and minimizing nonspecific toxicity. Many attempts were conducted to deliver PTX in a safer and more convenient manner. However, only a few PTX-delivery systems

such as Opaxio (poly glutamic acid–PTX) and Abraxane (albumin-bound paclitaxel) reached clinical trials or were approved by the FDA. There are many reasons that could be associated with failure of polymer conjugates in advanced preclinical studies and in clinical trials. Some of the limitations of the delivery systems could be overcome at the initials steps of design and synthesis of the conjugates. One such limitation could be associated with poor stability. An example is HPMA copolymer–PTX (PNU166945), in which PTX was attached to the HPMA copolymer through an ester bond. The linker was unstable under physiological conditions and underwent spontaneous hydrolysis from which PTX was released prematurely, and therefore induced the commonly observed toxicities of free PTX.<sup>15</sup> To face this challenge, we conjugated PTX with HPMA copolymer via a Phe-Lys-*p*-aminobenzyl carbonate (FK-PABC) linker that provided stable conjugation chemistry by the carbonate linkage and sustained release by cathepsin B. We also combined conjugation of both PTX and ALN to the same polymeric backbone. This dual targeting of PTX with a polymer and a bone targeting agent was designed to improve the pharmacokinetic and biodistribution of PTX to specifically accumulate in tumor sites

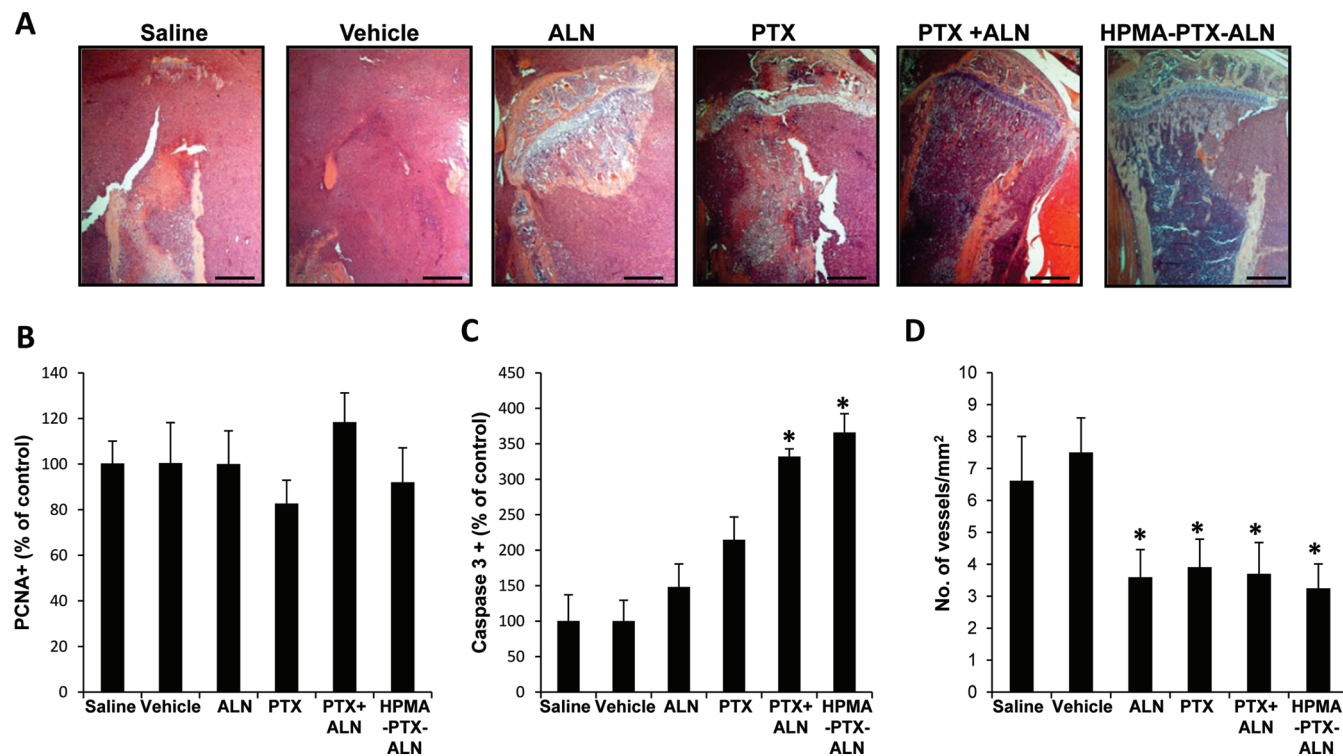


**Figure 5.** H&E and immunohistochemistry analysis of 4T1-mCherry mammary adenocarcinoma in the tibia treated with HPMA copolymer–PTX–ALN conjugate and the free drugs. (A) Representative histologic sections of 4T1-mCherry adenocarcinomas in the tibia. In control and in mice treated with free PTX or ALN, most of the cancellous bone in the primary and secondary spongiosae has been replaced by tumor cells that almost completely fill the bone marrow cavity. The cortical bone has also been destroyed completely; tumor cells have spread through the cortical bone into the surrounding soft tissues. In mice treated with HPMA copolymer–PTX–ALN conjugate cancer cells are present within the bone marrow cavity, however, most of the cortical bone is preserved. Scale bar represents 20  $\mu$ m. (B) Proliferation analysis, assessed by staining of PCNA (presented as % of positive staining of treatment/control). (C) Apoptosis analysis assessed by staining of caspase 3 (presented as % of positive staining of treatment/control), and (D) MVD assessed by vascular marker CD34 staining. \*P < 0.05 value of mice treated with HPMA copolymer–PTX–ALN conjugate was analyzed against saline control mice. \*P < 0.05 value of free PTX or combination of free PTX plus ALN was analyzed against control mice treated with PTX–vehicle.

within bones. Indeed, as reported previously, PTX was released from the conjugate solely by cathepsin B and HPMA copolymer–PTX–ALN demonstrated fast binding to the bone mineral HA.<sup>26</sup> In this study, we further evaluated the *in vitro* and *in vivo* performances of HPMA copolymer–PTX–ALN conjugate. The *in vitro* cytotoxicity study performed on both human MDA-MB-231 and murine 4T1 adenocarcinoma of the mammary cell lines showed that PTX, when bound to HPMA copolymer, retained its cytotoxicity. The fact that the conjugate is one log less toxic than free PTX may be attributed to the sustained release of PTX molecules from the conjugate, that is mediated by cathepsin B. An alternative option is that the polymer interferes with PTX activity. However, based on the results obtained from the *in vivo* experiments, showing enhanced efficacy by the conjugate at equivalent concentrations, we speculate that the sustained PTX release is likely the explanation. *Ex vivo* RBC lysis assay demonstrated that no hemolytic activity is related to HPMA copolymer–PTX–ALN conjugate at up to 5 mg/mL. In contrast, the commercial vehicle for PTX that contains Cremophor EL had significant hemolytic activity to RBC. Since no additive hemolysis effect was recorded in RBC incubated with combination of free PTX plus ALN, we speculate that it is probably caused by the Cremophor EL vehicle in which these drugs were dissolved, rather than the effect of the free drugs. In either case, conjugation of PTX with HPMA copolymer eliminated the need for the toxic Cremophor EL.

HPMA copolymer–PTX–ALN conjugate also demonstrated improved safety profile *in vivo*. Mice treated with the conjugate at low metronomic dosing schedule and MTD did not lose weight, and their WBC levels were comparable with those of saline treated mice. Interestingly, in both dosing schedules, only treatment with the combination of free ALN plus PTX had a significant effect, and caused body weight loss. WBC counts of mice treated with the low metronomic dose of PTX, the combination of free PTX plus ALN, and control of PTX–vehicle were below the levels of saline-treated control mice. In this case, PTX–vehicle decreased WBC counts and the effect seen in PTX and PTX plus ALN treatments might be due to PTX–vehicle effect, rather than the free drugs. Differently, MTD of PTX caused significant decrease in WBC levels, whereas treatment with both PTX–vehicle and combination of free PTX plus ALN had no effect over WBC counts. In these two assays different strains of mice were used. Mice treated with low metronomic dose were Balb/c, whereas mice treated with MTD were SCID, and it is well-known that different species of mice respond differently to treatments.<sup>39–42</sup> We therefore conclude that, whether the toxicity originated from the PTX–vehicle or from the PTX treatment, conjugation of PTX with HPMA copolymer eliminated the need for the toxic Cremophor, was soluble in water, and did not cause a decrease in WBC at any of the dosing schedules used.

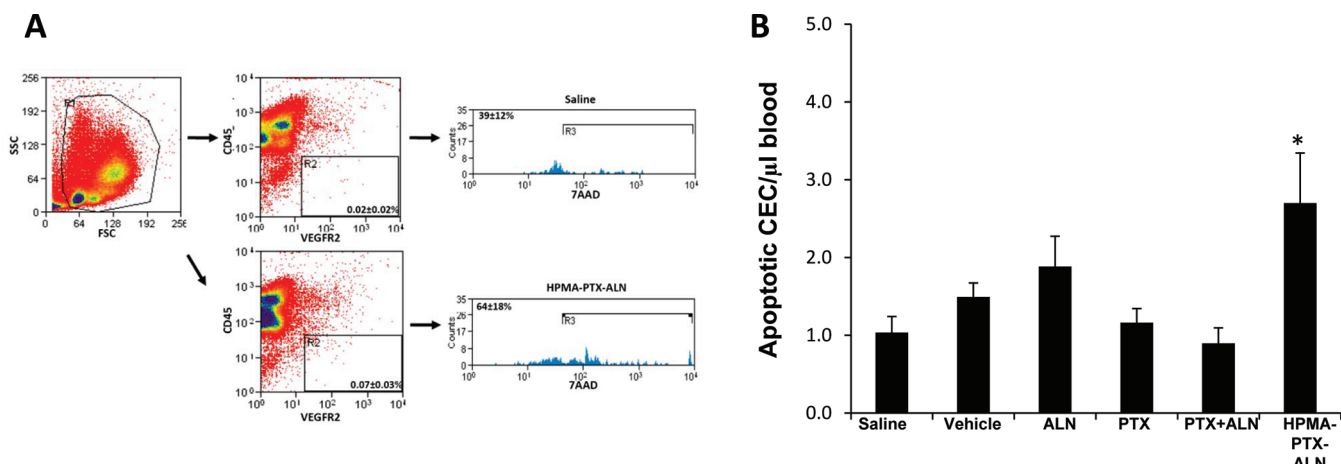


**Figure 6.** HPMA copolymer-PTX-ALN conjugate increases the apoptotic CEC counts. Mice bearing 4T1-mCherry tumors in the tibia were administered iv every other day with 15 mg/kg PTX, 9.5 mg/kg ALN, combination of free ALN plus PTX, HPMA copolymer-PTX-ALN conjugate at equivalent concentrations and with saline or PTX-vehicle as controls. On day 11, blood samples were collected and apoptotic CEC levels were measured using flow cytometry analysis. (A) Representative flow cytometry plots of apoptotic CEC analysis. Apoptotic CEC were determined as positive to VEGFR2 and negative or dim to CD45 surface markers (designated as R2 in the dot-plots). Cells from R2 region were also evaluated for their viability using the 7AAD dye (designated as R3 in the histograms). Flow cytometry plots of only saline and HPMA copolymer-PTX-ALN conjugate treated groups are presented. (B) Quantitative analysis of apoptotic CEC. The calculation of the number of apoptotic CEC in peripheral blood was based on the WBC of each mouse. \* $P < 0.05$  value of mice treated with HPMA copolymer-PTX-ALN conjugate was analyzed against saline control mice.

We previously reported the antiangiogenic properties of HPMA copolymer-PTX-ALN conjugate *in vitro*<sup>26</sup> and *in vivo*<sup>35</sup> when mice bearing PTX-resistant mCherry-DA3 murine mammary adenocarcinoma in the tibia were treated with low metronomic (antiangiogenic) dosing schedule of PTX. Treatment with the conjugate inhibited tumor growth by 40%, while treatment with the combination of free ALN plus PTX had no significant antitumor effect. As one of the goals of polymer-drug conjugation is to overcome drug resistance, in this mouse model, our HPMA copolymer-PTX-ALN conjugate overcame PTX resistance of DA3 cells.<sup>35</sup>

The antitumor efficacy of HPMA copolymer-PTX-ALN conjugate in the MTD schedule was here evaluated on mice bearing 4T1-mCherry mammary adenocarcinoma in the tibia. The conjugate exhibited the highest antitumor activity compared with free PTX or with combination of free PTX plus ALN at equivalent doses.

Immunohistochemistry analyses demonstrated significant increased apoptosis in both groups of treatment with HPMA copolymer-PTX-ALN conjugate or combination of free PTX plus ALN. These results suggest that the combined action of PTX and ALN in the absence of bone targeting for PTX is sufficient for the apoptotic effect. Moreover, the results obtained from immunohistochemistry of CD34 staining, showed similar significant reduced MVD in each free drug, when combined, and when conjugated with HPMA copolymer. From this data one can conclude that the additive effect of the combined free drugs is enough for antitumor effect with no benefit seen for bone targeting of PTX by the ALN and polymer conjugation. However, the superior tumor inhibition (Figures 5A, 5B) seen by the conjugate suggests that targeting PTX to bones using a polymer and ALN molecule is justified, and that it might be that other factors responsible for apoptosis, proliferation or recruitment of blood vessels, that were not analyzed in this study, are involved. Moreover, reduced toxicity seen in Figures 5C and SD definitely justifies the conjugation of both drugs with the polymer.

An increase in apoptotic CEC levels was recorded in HPMA copolymer-PTX-ALN-treated mice compared with control mice. Increase in apoptotic CEC usually indicates destruction of blood vessels. Therefore, we speculated that the increased circulation time, which was mediated by conjugation with the polymer, was the reason for the enhanced effect of the conjugate.

These findings, along with the inhibitory effect seen for reduced MVD by the conjugate, support our hypothesis that tumor growth inhibition of 4T1-mCherry mammary adenocarcinoma in the tibia was at least partly mediated by the antiangiogenic activity of HPMA copolymer-PTX-ALN conjugate.

The improved efficacy and reduced toxicity achieved by the conjugate is probably due to its improved pharmacokinetics that results in selective accumulation at the tumor site. PTX is released within hours, and this increases the exposure of tumor cells to free PTX.

In summary, HPMA copolymer-PTX-ALN conjugate demonstrated improved antitumor and antiangiogenic activity. Administration of the conjugate at both metronomic and high doses is safe and nontoxic. Exploiting the multivalency of polymers for targeting PTX to bones using ALN is novel and may introduce improved pharmacokinetics of polymer conjugates based on PTX.

## AUTHOR INFORMATION

### Corresponding Author

\*Department of Physiology and Pharmacology, Sackler School of Medicine, Tel Aviv University, Israel. Tel: +972-3-640 7427. Fax: +972-3-640 9113. E-mail: ronitsf@post.tau.ac.il

## ACKNOWLEDGMENT

This study was supported (in part) by Grant No. 5145-300000 from the Chief Scientist Office of the Ministry of Health, Israel, by THE ISRAEL SCIENCE FOUNDATION (Grant No. 1309/10), grants from Johnson & Johnson, matched by the Colton Family

Fund, Grant No. 2007347 given by the United States–Israel Binational Science Foundation (BSF) and The Israel Cancer Research Fund (ICRF) (RSF). We are grateful to the Marian Gertner Institute for Medical Nanosystems and The Cancer Biology Research Center for a Ph.D. fellowship (K.M.). This work is also supported by ISF and Marie Curie (under the FP7 EU program) given to Y.S. L.B. is supported by Fine, Jacobs and Israel Student Education Foundation studentships.

## ■ REFERENCES

- Caraglia, M.; Santini, D.; Marra, M.; Vincenzi, B.; Tonini, G.; Budillon, A. Emerging anti-cancer molecular mechanisms of aminobisphosphonates. *Endocr.-Relat. Cancer* **2006**, *13* (1), 7–26.
- Colleoni, M.; O'Neill, A.; Goldhirsch, A.; Gelber, R. D.; Bonetti, M.; Thurlimann, B.; Price, K. N.; Castiglione-Gertsch, M.; Coates, A. S.; Lindtner, J.; Collins, J.; Senn, H. J.; Cavalli, F.; Forbes, J.; Gudgeon, A.; Simoncini, E.; Cortes-Funes, H.; Veronesi, A.; Fey, M.; Rudenstam, C. M. Identifying breast cancer patients at high risk for bone metastases. *J. Clin. Oncol.* **2000**, *18* (23), 3925–35.
- Bhalla, K. N. Microtubule-targeted anticancer agents and apoptosis. *Oncogene* **2003**, *22* (56), 9075–86.
- Arbuck, S. G.; Dorr, A.; Friedman, M. A. Paclitaxel (Taxol) in breast cancer. *Hematol. Oncol. Clin. North Am.* **1994**, *8* (1), 121–40.
- Sanfilippo, N. J.; Taneja, S. S.; Chachoua, A.; Lepor, H.; Formenti, S. C. Phase I/II study of biweekly paclitaxel and radiation in androgen-ablated locally advanced prostate cancer. *J. Clin. Oncol.* **2008**, *26* (18), 2973–8.
- Cetnar, J. P.; Malkowicz, S. B.; Palmer, S. C.; Wein, A. J.; Vaughn, D. J. Pilot trial of adjuvant paclitaxel plus estramustine in resected high-risk prostate cancer. *Urology* **2008**, *71* (5), 942–6.
- Michaud, L. B.; Valero, V.; Hortobagyi, G. Risks and benefits of taxanes in breast and ovarian cancer. *Drug Saf.* **2000**, *23* (5), 401–28.
- Wang, J.; Lou, P.; Lesniewski, R.; Henkin, J. Paclitaxel at ultra low concentrations inhibits angiogenesis without affecting cellular microtubule assembly. *Anticancer Drugs* **2003**, *14* (1), 13–9.
- Pasquier, E.; Carre, M.; Pourroy, B.; Camoin, L.; Rebai, O.; Briand, C.; Braguer, D. Antiangiogenic activity of paclitaxel is associated with its cytostatic effect, mediated by the initiation but not completion of a mitochondrial apoptotic signaling pathway. *Mol. Cancer Ther.* **2004**, *3* (10), 1301–10.
- Gelderblom, H.; Verweij, J.; Nooter, K.; Sparreboom, A. Cremophor EL: the drawbacks and advantages of vehicle selection for drug formulation. *Eur. J. Cancer* **2001**, *37* (13), 1590–8.
- Orr, G. A.; Verdier-Pinard, P.; McDaid, H.; Horwitz, S. B. Mechanisms of Taxol resistance related to microtubules. *Oncogene* **2003**, *22* (47), 7280–95.
- Horwitz, S. B.; Cohen, D.; Rao, S.; Ringel, I.; Shen, H. J.; Yang, C. P. Taxol: mechanisms of action and resistance. *J. Natl. Cancer Inst. Monogr.* **1993**, *15*, 55–61.
- Li, C.; Newman, R. A.; Wu, Q. P.; Ke, S.; Chen, W.; Hutto, T.; Kan, Z.; Brannan, M. D.; Charnsangavej, C.; Wallace, S. Biodistribution of paclitaxel and poly(L-glutamic acid)-paclitaxel conjugate in mice with ovarian OCa-1 tumor. *Cancer Chemother. Pharmacol.* **2000**, *46* (5), 416–22.
- Singer, J. W. Paclitaxel polyglumex (XYOTAX, CT-2103): a macromolecular taxane. *J. Controlled Release* **2005**, *109* (1–3), 120–6.
- Meerum Terwogt, J. M.; ten Bokkel Huinink, W. W.; Schellens, J. H.; Schot, M.; Mandjes, I. A.; Zurlo, M. G.; Rocchetti, M.; Rosing, H.; Koopman, F. J.; Beijnen, J. H. Phase I clinical and pharmacokinetic study of PNU166945, a novel water-soluble polymer-conjugated prodrug of paclitaxel. *Anticancer Drugs* **2001**, *12* (4), 315–23.
- Duncan, R. Polymer conjugates as anticancer nanomedicines. *Nat. Rev. Cancer* **2006**, *6* (9), 688–701.
- Vicent, M. J.; Greco, F.; Nicholson, R. I.; Paul, A.; Griffiths, P. C.; Duncan, R. Polymer therapeutics designed for a combination therapy of hormone-dependent cancer. *Angew. Chem., Int. Ed.* **2005**, *44* (26), 4061–6.
- Haag, R.; Kratz, F. Polymer therapeutics: concepts and applications. *Angew. Chem., Int. Ed.* **2006**, *45* (8), 1198–215.
- Miller, K.; Satchi-Fainaro, R. Polymer Therapeutics: From novel concepts to clinical applications. In *Wiley Encyclopedia of Chemical Biology*; Civjan, N. R., J. W. S., Inc.: Hoboken, 2009; Vol. 3, pp 783–99.
- Duncan, R.; Ringsdorf, H.; Satchi-Fainaro, R. Polymer therapeutics—polymers as drugs, drug and protein conjugates and gene delivery systems: past, present and future opportunities. *J. Drug Targeting* **2006**, *14* (6), 337–41.
- Greco, F.; Vicent, M. J. Polymer-drug conjugates: current status and future trends. *Front. Biosci.* **2008**, *13*, 2744–56.
- Maeda, H.; Wu, J.; Sawa, T.; Matsumura, Y.; Hori, K. Tumor vascular permeability and the EPR effect in macromolecular therapeutics: a review. *J. Controlled Release* **2000**, *65* (1–2), 271–84.
- Pan, H.; Sima, M.; Kopeckova, P.; Wu, K.; Gao, S.; Liu, J.; Wang, D.; Miller, S. C.; Kopecek, J. Biodistribution and pharmacokinetic studies of bone-targeting N-(2-hydroxypropyl)methacrylamide copolymer-alendronate conjugates. *Mol. Pharmaceutics* **2008**, *5* (4), 548–58.
- Wang, D.; Sima, M.; Mosley, R. L.; Davda, J. P.; Tietze, N.; Miller, S. C.; Gwilt, P. R.; Kopeckova, P.; Kopecek, J. Pharmacokinetic and biodistribution studies of a bone-targeting drug delivery system based on N-(2-hydroxypropyl)methacrylamide copolymers. *Mol. Pharmaceutics* **2006**, *3* (6), 717–25.
- Uludag, H. Bisphosphonates as a foundation of drug delivery to bone. *Curr. Pharm. Des.* **2002**, *8* (21), 1929–44.
- Miller, K.; Erez, R.; Segal, E.; Shabat, D.; Satchi-Fainaro, R. Targeting bone metastases with a bispecific anticancer and antiangiogenic polymer-alendronate-taxane conjugate. *Angew. Chem., Int. Ed.* **2009**, *48* (16), 2949–54.
- Strojanik, T.; Kos, J.; Zidanik, B.; Golouh, R.; Lah, T. Cathepsin B immunohistochemical staining in tumor and endothelial cells is a new prognostic factor for survival in patients with brain tumors. *Clin. Cancer Res.* **1999**, *5* (3), 559–67.
- Lah, T. T.; Kalman, E.; Najjar, D.; Gorodetsky, E.; Brennan, P.; Somers, R.; Daskal, I. Cells producing cathepsins D, B, and L in human breast carcinoma and their association with prognosis. *Hum. Pathol.* **2000**, *31* (2), 149–60.
- Sinha, A. A.; Wilson, M. J.; Gleason, D. F.; Reddy, P. K.; Sameni, M.; Sloane, B. F. Immunohistochemical localization of cathepsin B in neoplastic human prostate. *Prostate* **1995**, *26* (4), 171–8.
- Foekens, J. A.; Kos, J.; Peters, H. A.; Krasovec, M.; Look, M. P.; Cimerman, N.; Meijer-van Gelder, M. E.; Henzen-Logmans, S. C.; van Putten, W. L.; Klijn, J. G. Prognostic significance of cathepsins B and L in primary human breast cancer. *J. Clin. Oncol.* **1998**, *16* (3), 1013–21.
- Ofek, P.; Fischer, W.; Calderon, M.; Haag, R.; Satchi-Fainaro, R. In vivo delivery of small interfering RNA to tumors and their vasculature by novel dendritic nanocarriers. *FASEB J.* **2010**, *24* (9), 3122–34.
- Weidner, N.; Semple, J. P.; Welch, W. R.; Folkman, J. Tumor angiogenesis and metastasis—correlation in invasive breast carcinoma. *N. Engl. J. Med.* **1991**, *324* (1), 1–8.
- Shaked, Y.; Bertolini, F.; Man, S.; Rogers, M. S.; Cervi, D.; Foutz, T.; Rawn, K.; Voskas, D.; Dumont, D. J.; Ben-David, Y.; Lawler, J.; Henkin, J.; Huber, J.; Hicklin, D. J.; D'Amato, R. J.; Kerbel, R. S. Genetic heterogeneity of the vasculogenic phenotype parallels angiogenesis; Implications for cellular surrogate marker analysis of antiangiogenesis. *Cancer Cell* **2005**, *7* (1), 101–11.
- Bilensoy, E.; Gurkaynak, O.; Dogan, A. L.; Hincal, A. A. Safety and efficacy of amphiphilic beta-cyclodextrin nanoparticles for paclitaxel delivery. *Int. J. Pharm.* **2008**, *347* (1–2), 163–70.
- Paula Ofek, K. M.; Eldar-Boock, Anat; Polyak, Dina; Segal, Ehud Ronit Satchi-Fainaro. Rational Design of Multifunctional Polymer Therapeutics for Cancer Theranostics. *Isr. J. Chem.* **2010**, *50* (2), 185–201.
- Bertolini, F.; Mancuso, P.; Braidotti, P.; Shaked, Y.; Kerbel, R. S. The multiple personality disorder phenotype(s) of circulating endothelial cells in cancer. *Biochim. Biophys. Acta* **2009**, *1796* (1), 27–32.

(37) Bertolini, F.; Shaked, Y.; Mancuso, P.; Kerbel, R. S. The multifaceted circulating endothelial cell in cancer: towards marker and target identification. *Nat. Rev. Cancer* **2006**, *6* (11), 835–45.

(38) Shaked, Y.; Tang, T.; Woloszynek, J.; Daenen, L. G.; Man, S.; Xu, P.; Cai, S. R.; Arbeit, J. M.; Voest, E. E.; Chaplin, D. J.; Smythe, J.; Harris, A.; Nathan, P.; Judson, I.; Rustin, G.; Bertolini, F.; Link, D. C.; Kerbel, R. S. Contribution of granulocyte colony-stimulating factor to the acute mobilization of endothelial precursor cells by vascular disrupting agents. *Cancer Res.* **2009**, *69* (19), 7524–8.

(39) Tyan, M. L. Effect of age on the intrinsic regulation of murine hemopoiesis. *Mech. Ageing Dev.* **1982**, *19* (1), 15–20.

(40) Danieyko-Osman, M.; Mietkiewski, E. Erythropoietic effect of ultraviolet radiation in blind rats in comparison with control seeing rats. *Acta Physiol. Pol.* **1982**, *33* (3), 169–77.

(41) Chai, C. K.; Lerner, C. Hemopoietic stem cell reconstitution from mouse strains differing greatly in leukocyte production. *Exp. Hematol.* **1980**, *8* (7), 880–3.

(42) Oghiso, Y.; Yamada, Y. Strain differences in carcinogenic and hematopoietic responses of mice after injection of plutonium citrate. *Radiat. Res.* **2000**, *154* (4), 447–54.